COMBINATORIAL CHARACTERIZATION OF PHOTOPOLYMERIZABLE COMPOSITES: EFFECT OF FILLER TYPE AND CONTENT ON PROPERTIES

Sheng Lin-Gibson,[*,a] *Lipiin Sung,*[b] *Aaron M. Forster,*[b] *Haiqing Hu,*[b] *and Nancy J. Lin,*[a]

[a]Polymers Division, National Institute of Standards and Technology, Gaithersburg, MD 20899-8543, USA

[b]Materials and Construction Research Division, National Institute of Standards and Technology, Gaithersburg, MD 20899-8615, USA

Official contribution of the National Institute of Standards and Technology; not subject to copyright in the United States

Introduction

Dental composites are complex systems comprised of a photopolymerizable binary or ternary resin mixture filled with inorganic particles. As such, a large number of chemical and processing parameters influence their properties.[1] Dental composites must meet a stringent series of performance benchmarks to achieve clinical acceptance. Because of the complexity in composite formulation, systematic variation of formulation parameters and subsequent screening of multiple properties on a large number of samples is time consuming, laborious, and often impractical. High-throughput and combinatorial (HT&C) methods using either continuous gradient or discrete array libraries have the advantages of faster data acquisition, wider examination of experimental variables, equal processing conditions for a given specimen, and greater experimental statistics over traditional one-at-a-time methods.

We have been utilizing HT&C methods to screen multiple properties of dental polymers.[2-4] Our previous studies focused on 2-dimensional (2D) composition arrays and degree of conversion (DC) gradients of dental polymers using a monomer system consisting of binary mixtures of bisphenol-A-glycidyl dimethacrylate (BisGMA) and triethylene glycol dimethacrylate (TEGDMA). We have also studied the biocompatibility of dental polymers and composites using 2D platforms. In the current study, we investigated the effects of filler size and concentration on various chemical, physical, and mechanical properties, in addition to biological properties. All measurements were performed on the same samples – the 2D specimens – thus allowing direct comparison of the data.

Experimental

Materials[*] Resins BisGMA and TEGDMA were obtained from Esstech Inc. Photoinitiator system components, camphorquinone (CQ) and ethyl 4-*N*,*N*-dimethylaminobenzoate (4E), were purchased from Aldrich Corp. The SP 345 silane glass filler (SG, 0.70 μm average diameter) and fumed amorphous silica filler (OX50, 0.04 μm average diameter) were provided by the L.D. Caulk Company. Cell culture reagents were purchased from Invitrogen Corp., unless otherwise noted. All reagents were used as received.

Composite Preparation. BisGMA and TEGDMA (mass ratio = 50:50) were activated for blue light photopolymerization with 0.2 % CQ and 0.8 % 4E (by mass) and stored in the dark until use. The SG and OX50 fillers were mixed into the activated resin following the formulations shown in Table 1. The 2D specimens consisted of a discrete array in composite formulation (individual stripes) along one axis with an orthogonal gradient in methacrylate conversion.

The specimens were fabricated by adapting procedures previously used for specimens of unfilled polymers.[4] Briefly, the five composite pastes were sandwiched in a mold consisting of two glass slides, a polyester release film, and a poly(dimethylsiloxane) spacer (thickness ≈ 1.5 mm) with five channels. The conversion gradients were generated by first placing the assembly 10 cm beneath a light source (120 V, 250 W). The irradiation intensity from this source decreases exponentially, with the highest irradiation occurring directly underneath the center of the light source. The sample was positioned with one edge directly under the center of the light source and irradiated for 15 s per side. Then, a shield was used to partially cover the sample during a further exposure of 1 min per side. Specimens were stored in the dark for 24 h prior to characterization. A notch was made across the DC gradient at the high conversion end and defined as the zero position.

Table 1. Composite formulations

Formulation	*Activated Resin (% by mass)*	*SG (% by mass)*	*OX50 (% by mass)*
S1	35	65	0
S2	50	50	0
S3	50	45	5
S4	65	30	5
S5	80	15	5

Characterization. Transmission near infrared (NIR) spectroscopy was performed using a Nicolet Magna 550 Fourier transform infrared (FTIR) spectrometer (Madison, WI). The NIR spectra in the region of 7000 cm^{-1} to 4000 cm^{-1} were acquired from 32 averaged scans at 6 cm^{-1} resolution. The relative uncertainty associated with the NIR measurements is 3 %.

Surface morphology and RMS (root-mean-square) surface roughness were measured using a reflection laser scanning confocal microscope (LSCM). A 10X and a 50X objective were used to scan an area of 921.4 μm x 921.4 μm and 184.3 μm x 184.3 μm, respectively.

Depth sensing indentation (DSI) measurements were performed using a MTS Nanoinstruments NanoXP instrument (Oak Ridge, TN) equipped with a 10 μm radius, 90° diamond cone indenter. The contact stiffness between the sample and tip was measured by superposing a small oscillation (45 Hz, 5 nm) over the load profile. Three indents (n = 3) were measured at each location. The standard uncertainty associated with DSI measurements is 5 %.

The surface of each composite was scratched parallel to the conversion gradient (n = 3) and within 1 mm of each indent location using the same indenter (10 μm radius, 90° diamond cone tip). A progressive-load scratch method was used to produce three 400 μm scratches parallel to the curing gradient from 0 mm to 50 mm at 10 mm intervals. LSCM (150X objective) was used to characterize the scratch morphology, including scratch width, full depth (D_f), and the scratch damage patterns. The scratch width (W_p) was defined as the peak-to-peak distance perpendicular to the scratch length. The W_p/D_f ratio was also calculated. The standard uncertainty associated with the scratch measurements is 5 %.

Viability of macrophages on the samples was assessed as previously described.[3,4] Briefly, RAW 264.7 murine macrophage-like cells (American Type Culture Collection, ATCC TIB-71) were cultured in Roswell Park Memorial Institute (RPMI) 1640 growth medium containing 10 % (by volume) heat-inactivated fetal bovine serum. Gradient substrates were sterilized using ethylene oxide gas and aged in phosphate buffered saline (PBS) for 7 d. Cells were seeded directly onto the substrates and onto negative control tissue culture polystyrene plates for a final cell density of 2.5 x 10^4 cells/cm^2. After culturing for 24 h in a humidified incubator (37 °C, 5 % CO_2 by volume), cells were stained for viability using growth medium containing calcein acetoxymethyl ester (calcein AM, live cells, 2 μmol/L), ethidium homodimer-1 (EthD-1, dead cells, 2 μmol/L), and Hoechst 33342 (H33342, all cells, 10 μmol/L) and imaged on a Leica DMA epifluorescence microscope.

Results and Discussion

With the addition of fillers, the first noticeable effect was that composites that were cured with reduced irradiation time and intensity exhibited an increased surface roughness at lower DC. Projection views of the surface roughness, generated using confocal microscopy, revealed a generally smooth surface at high DC that became progressively rougher with decreasing DC (Fig. 1). The same trend was observed for all compositions and using two different microscope objectives. The mechanism for generating the roughness gradient is likely associated with the photopolymerization protocol and is the subject of further investigation.

[*] Certain equipment, instruments or materials are identified in this paper to adequately specify the experimental details. Such identification does not imply recommendation by the National Institute of Standards and Technology, nor does it imply the materials are necessary the best available for the purpose.

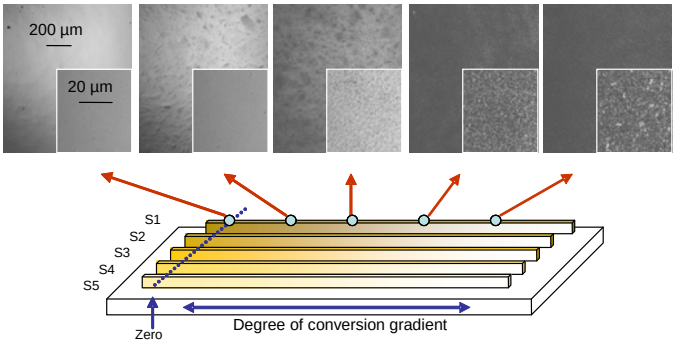

Figure 1. The gradient samples consisted of five discrete compositions each varying in DC. A) LSCM (10X objective, and inset 50X objective) was used to image the surface roughness.

The DC and modulus (E) maps for the composition-conversion gradient are illustrated in Fig. 2. A higher DC was achieved with increased exposure to irradiation for all compositions. For the current system, S1 had a slightly lower DC when compared to other compositions ($P < 0.05$), but the deviation was small and primarily occurred at position 0 mm. S2 thru S5 were statistically identical for any given position along the conversion gradient. The corresponding modulus map for the gradient sample shows a profile similar to the DC map. The modulus of S1 (highest filler loading) is significantly higher than that of the other compositions throughout the entire conversion gradient. This trend is observed despite the fact that S1 had a slightly lower DC than the other compositions, indicating the importance of utilizing a high filler loading to increase the elastic modulus. Although S2, S4, and S5 had different filler loading and types, the modulus at the highest DC was not significantly different among these formulations. The results indicate that at filler loadings of 50 % (by mass) and below, the modulus is governed by the matrix polymer.

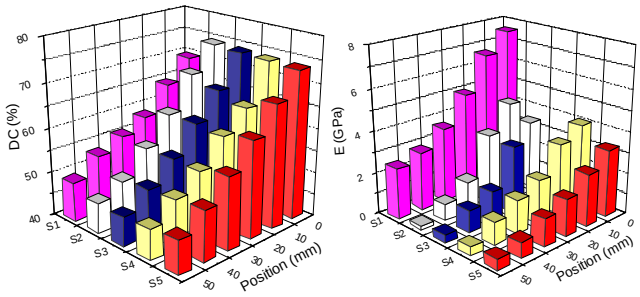

Figure 2. Degree of conversion (left) and modulus (right) as a function of composition and irradiation (position).

Progressive load scratch tests were used to characterize the response of the 2D array sample to scratch damage. The entire scratch profile was examined by confocal microscopy as a function of position (Fig. 3A). All composites exhibited two modes of deformation at high DCs (DC ≥ 65 %), e.g., elastic and plastic. Below a DC of 65 %, the scratch resulted in three modes of deformation with the addition of fracture deformation. Elastic deformation was observed at low scratch loads whereby the composite was able to fully recover after removal of the normal load. A larger scratch load resulted in elastic and plastic deformation with the plastic deformation manifested as ductile grooving that transitioned into ploughing with increasing applied normal force. The 3D profiles of the scratches at high load, imaged using confocal microscopy via the 150X objective, showed fractures extending from the walls of the scratch at low DC (Fig. 3B, arrows). In addition, the surface roughness increased with decreasing DC, similar in magnitude to the features observed using the 50X objective. From the depth profiles, the scratch deformation was quantified in terms of full depth (D_f), peak-to-peak position (W_p), and their ratio (W_p/D_f). For all composites, D_f increased as DC decreased. The filler concentration was inversely related to W_p at high DC (0 mm position), as the scratches were wider for composites with less filler. With the exception of the lowest DC of S1 (40 mm) and the highest DC for S2 (0 mm), W_p increased with decreased DC. Another useful analysis method for quantifying the material properties is to compare the initial penetration curves with the residual penetration curves from scratch measurements. The residual penetration depth curve reflects residual plastic and any long time viscoelastic deformation.

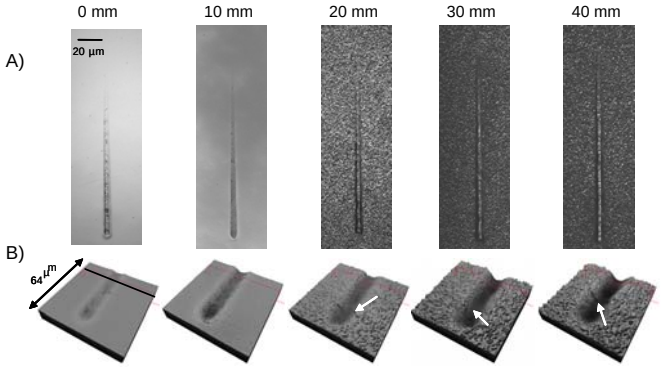

Figure 3. Progressive load scratches (400 µm in length) measured along the conversion gradient for a single composition (S2). A) LSCM image of the scratch at each position, B) 3D LSCM projection (150X objective) of the 50 mN normal force section of the scratches (arrows indicate fractures).

After characterizing the surface mechanics and physical properties using the 2D platforms, the cell response was also investigated on the same platforms. To evaluate the effects of the surface properties on the biological response, RAW 264.7 macrophages were cultured directly on the 2D samples. Macrophages are inflammatory cells that are involved in the first line of defense against foreign objects in the body and are therefore useful when evaluating cell-material interactions. The viability stain revealed differences in cell response as a function of composition and DC (results not shown). Macrophage viability decreased at low DC only for S4 and S5, the compositions with the lowest filler content. Since the neat polymer has also been shown to be toxic at low DC, cell death at lower conversions in S4 and S5 is due to the increased presence of undercured polymer. Cell density also decreased as a function of decreasing DC for S4 and S5.

Conclusions

The 2D array platform presented in the current study is amenable for screening multiple material properties and biological response on the same sample. This study highlights the use of LSCM, DSI, and scratch testing in conjunction with the gradient substrates to evaluate surface topology and mechanical properties. In addition, cytotoxicity was assessed, and results were compared with the physical and mechanical properties of the substrate. For each substrate, composition was varied discretely by changing the filler content and filler type (with or without nanofiller), and continuous gradients in degree of conversion were fabricating during photopolymerization. Overall, the results suggest that filler mass fraction, the presence of nanofiller, and the degree of conversion work in concert to affect the surface properties, mechanical properties, and cell response. The combinatorial approach was advantageous for this study, as it provided a more thorough evaluation of the materials and enabled the screening of a number of material parameters.

Acknowledgements. Financial support was provided through an NIDCR/NIST Interagency Agreement Y1-DE-7005-01. The dental resins and fillers were kindly donated by Esstech Inc and L.D. Caulk Company, respectively.

References

(1) Ferracane JA. Materials in Dentistry: Principles and Application. Second edition ed. Baltimore, MD: Lippincott Williams & Wilkins; 2001.
(2) Lin-Gibson S, Landis FA, Drzal PL.*Biomaterials* **2006**;27:1711-1717.
(3) Lin NJ, Bailey LO, Becker ML, Washburn NR, Henderson LA. *Acta Biomaterialia* **2007**;3:163-173.
(4) Lin NJ, Drzal PL, Lin-Gibson S. *Dental Materials* **2007**;23:1211-1220.